

Electrochemically-induced formation of Cytochrome c oligomers at soft interfaces

Eva Alvarez de Eulate,^[a] Shane O'Sullivan^[a] and Damien W. M. Arrigan^{*[a]}

The formation of cytochrome *c* oligomers was induced at liquid-gel and liquid-liquid interfaces via electroadsorption. At an optimum interfacial potential ($E_{ads} = 0.975$ V), the protein was accumulated at these soft interfaces. It was found that as the concentration of adsorbed protein increased, a single voltammetric peak evolved into double and triple peaks ($t_{ads} = 300$ s). Analysis of the protein accumulated at the interfaces by polyacrylamide gel electrophoresis indicated the presence of oligomeric species corresponding to dimers (~27 kD), trimers (~35 kD) and even larger species (> 250 kD) after prolonged electroadsorption ($t_{ads} = 2$ h) at macro-scale soft interfaces. Accordingly, it was possible to electrochemically induce oligomerisation at these soft interfaces which can be tuned via experimental factors such as interfacial potential difference, electroadsorption time, bulk solution concentration. These results suggest the use of electrochemistry at soft interfaces as a strategy for investigation of protein oligomerisation and its inhibition.

1. Introduction

Cytochrome *c* (cyt *c*) is a globular protein containing a covalently bound haem group^[1] which is known to form oligomers under certain conditions, such as treatment with organic solvents and with acids,^[2] although the mechanism of this process is not fully understood. A recent study has determined the crystal structures of dimeric and trimeric cyt *c* complexes, which has shown that they polymerise through domain swapping of C-terminal helices from one cyt *c* molecule to another.^[3] This study showed that the methionine 80 residue was dissociated from the haem group in order to facilitate domain swapping. Generally, factors such as amino acid sequence, charge, unfolded regions and hydrophobicity contribute to fibril formation.^[4] Under conditions^[4] such as high temperature in basic^[1a] or acidic media,^[5] or in the presence of specific reagents,^[6] some proteins convert from their native form into highly ordered fibrillar aggregates.^[4] The formation of fibrils has been associated with many diseases and neurodegenerative disorders, such as Alzheimer's disease, Huntington's disease, Parkinson's disease, type II diabetes, Spongiform encephalopathies and spinocerebellar ataxia, just to name a few.^[1a, 4, 7] Many globular proteins can form amyloid fibrils

under conditions which induce denaturation.^[8] It has also been proposed that the oligomeric intermediates of fibril formation are the species responsible for neurodegenerative effects.^[9]

Recent electrochemical studies at solid-liquid interfaces have aimed to unravel the mechanism of early stages of peptide self-assembly into fibrillar amyloids where toxic soluble aggregates are formed. Protein-catalyzed hydrogen evolution, interfacial capacitive changes and the use of β -sheet-binding dyes (e.g. Congo Red and Thioflavin T) are some examples of the methods employed.^[10] Furthermore, Ferapontova *et al.* have mapped electrochemically and via atomic force microscopy the fibril formation of amyloid β (A β) peptides by tracking the oxidation of tyrosine in position 10 (Tyr10). This approach allowed the discrimination of various A β 42 states, as Tyr10 is hidden in aggregate states.^[11] As amyloids are known to form in extracellular space and destabilize the cell membrane,^[7b] the liquid-liquid interface may provide an experimental model for the investigation of oligomer and fibril formation. The interface between two immiscible electrolyte solutions (ITIES) provides a platform for the investigation into the behaviour of macromolecules based on ion transfer across the interface.^[12] This has been employed to investigate a range of biologically-relevant molecules such as amino acids and peptides^[13] as well as various proteins, e.g. haemoglobin,^[14] cyt *c*,^[15] myoglobin^[16] and lysozyme.^[17] The primary objective of many investigations is to use electrochemistry at the ITIES as a basis for detection, so that the focus tends to lie in the areas of achieving lower detection limits by miniaturising the interface,^[18] overcoming problems associated with sensing in complex matrices and selectivity issues by employing ionophores,^[19] or developing more complex flow cell techniques to improve assay performance.^[20] There has been less focus on understanding the complex behaviour of proteins at such interfaces. For instance, the effects of protein structure, stability, size, charge and hydrophobicity on the electrochemical behaviour are less well understood. Pioneering work on interfacial electron transfer across the ITIES between cyt *c* and 1,1'-dimethylferrocene^[15] and interfacial cyt *c* complexation with anionic surfactants have demonstrated this complexity.^[21] It has also been shown that denaturation of haemoglobin leads to an attenuated electrochemical response at the ITIES.^[22] A recent study using spectroscopic methods showed that the structure and conformation of α -lactalbumin changed significantly when adsorbed at the oil-water interface,^[23] although no electrochemical control was used. It has also been reported that proteins undergo a charge regulation process when adsorbed at such interfaces, indicating that the charge of the protein in bulk is not necessarily indicative of the charge of the adsorbed molecules.^[24] Hartvig *et al.* identified protein-ligand complexes at chemically polarized interfaces by biphasic electrospray ionization-mass spectrometry (BESI-MS) and showed that electrostatic interactions influenced interfacial adsorption.^[25] However, protein-protein interactions, which are likely to play a key role in behaviour at the oil - water interface, and therefore the

[a] Dr. Eva Alvarez de Eulate, Dr. Shane O'Sullivan and Prof. Damien W. M. Arrigan
Nanochemistry Research Institute & Department of Chemistry
Curtin University
GPO Box U1987, Perth, Western Australia, Australia 6845
E-mail: d.arrigan@curtin.edu.au

Supporting information for this article is given via a link at the end of the document.

impact of interfacial concentration of adsorbed protein have not been addressed. Recently, the method of adsorptive stripping voltammetry (AdSV) was applied to achieve low limits of detection for lysozyme at an array of micrometre-sized ITIES (μ ITIES array)^[26] and subsequently combined with electrostatic spray ionization-mass spectrometry (ESTASI-MS) to analyse protein structural changes.^[27] The AdSV method effectively pre-concentrates the protein at the interface via a potential-controlled electroadsorption for a fixed time, providing an enhanced current response to the protein during the subsequent desorption step. Application of this AdSV approach to cyt *c* produced some unusual results, which are the subject of this work.

The aim of this study was to investigate the electroactivity of cyt *c* at a μ ITIES array and to examine whether protein oligomerisation occurred. By controlling electroadsorption at the ITIES, the interfacial concentration can be manipulated to conditions perhaps conducive to oligomerisation. Cyt *c* is a model protein for this investigation because it is electroactive at the ITIES, presents multiple conformational states, and is known to polymerise in water.

2. Results and Discussion

2.1 Cytochrome *c* voltammetry at the μ ITIES array

As shown previously for other proteins,^[16, 26a] the detection of cyt *c* at the ITIES consists of facilitated transfer of organic phase electrolyte anions by the cationic protein, followed by interfacial adsorption of the protein-anion complex (Figure 1, regions 1 and 2). Voltammetry was carried out with the protein present in an acidic aqueous phase to ensure it is fully protonated, in line with previous studies.^[16, 26a] Such conditions are quite different to those experienced in nature, but are the optimum conditions for protein detection via electrochemistry at the ITIES.^[16,17,18a,26] The adsorption of cyt *c* at water/gelled-1,6-dichlorohexane (w/gelled-DCH) μ ITIES array was achieved by imposing a potential difference ($\Delta\phi^0 E$) across the ITIES to promote protein adsorption.

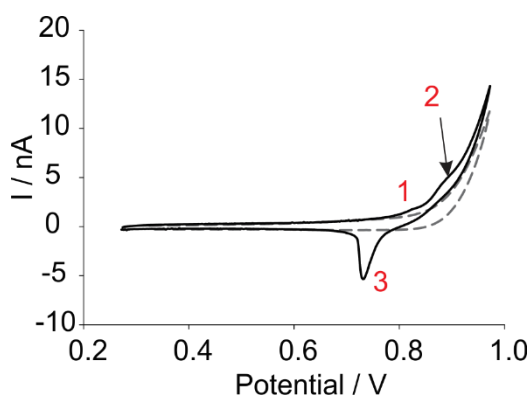


Figure 1. CV of 10 μ M cyt *c* in 10 mM HCl (solid line) and without cyt *c* in 10 mM HCl (dashed line) at w/DCH microinterface array; potential range from 0.250 V to 0.975 V and scan rate 5 mV s⁻¹. Mechanism steps: 1) adsorption pre-wave, 2) complexation by facilitated transfer of organic anion, and 3) desorption.

Subsequently, the interfacially-accumulated protein can be stripped (desorbed, 3 in Figure 1) by scanning to lower potentials, which is the basis of the AdSV method. In this respect, cyt *c*

behaves similarly to other proteins examined by this approach. Hence, the interfacial coverage can be evaluated directly from the electrochemical measurement.

To determine the optimum adsorption conditions, AdSV was implemented at various interfacial potential differences (E_{ads}) and adsorption times (t_{ads}) (Figure 2), as reported for lysozyme.^[26a] These experiments were conducted at low pH, so as to fully protonate cyt *c* ($pH < pI$, $pI = 10.0-10.5$)^[28] to maximize the facilitated transfer of organic phase anions. The adsorption potentials were varied between 0.6 V and 1.0 V and followed by the voltammetric desorption scan to lower potentials (Figure 2a). As can be seen from Figure 2b, the stripping peak current is dependent on the initial applied potential. An optimal response was obtained at 0.975 V, which resulted in a peak current of -4.8 nA. It can be seen from Figure 2b, that below 0.875 V no voltammetric response was obtained for cyt *c*, due to insufficient amounts of adsorbed protein at the interface, whereas above 0.975 V the response was diminished as background electrolyte transfer processes dominate at this potential region, such as organic electrolyte anion transfer without complexation to the protein.

The influence of adsorption time on the electrochemical response of cyt *c* was also investigated by using AdSV. This involved applying a fixed adsorption potential ($E_{ads} = 0.975$ V) for various set times ($t_{ads} = 0$ s – 1800 s) so that the protein was efficiently pre-concentrated at the interface. The protein was then subsequently “stripped” from the interface by its desorption when the applied potential was swept lower values.^[26a] Figure 2c shows the resulting stripping voltammograms obtained in the presence of 1 μ M cyt *c* following various adsorption times. Figure 2d shows a plot of the stripping peak current versus adsorption time. As previously stated, the AdSV peak current at -0.67 V is due to protein desorption and back transfer of the organic anion from the aqueous phase to the organic phase. The peak current values, Figure 2d, are shown to increase with increasing adsorption time up to a plateau value, indicating a saturation of available adsorption capacity at the ITIES. However, closer inspection of Figure 2c indicates that some unexpected events occur that are not encapsulated in the peak current data. It can be clearly seen that the background current in the potential region where no charge transfer processes occur (Figure 2c, from 0.6 V to 0.4 V) is changing dramatically with increasing adsorption time, from -0.75 nA at 0 s, to -5.57 nA at 1800 s adsorption time. This is indicative of a change in the interfacial composition, perhaps to non-desorbed protein. Furthermore, a small shoulder begins to emerge on the desorption peak at 0.65 V following adsorption times that exceed 600 s. These changes indicate new processes which are surface concentration (interfacial coverage) dependent, as adsorption time is linked directly to interfacial protein concentration.

AdSV of cyt *c* was also performed using fixed adsorption times (0, 60, 120, 300 s) while the concentration of the protein ($C_{cyt\ c}$) was varied (0.01 – 10.0 μ M), Figure 2e-f. The minimum measurable reverse peak was observed at 0.5 μ M for 0, 60 and 120 s adsorption times, whereas at 300 s adsorption time a peak was measurable at 0.25 μ M, Figure 2f. At short adsorption times ($t_{ads} = 0 - 120$ s), the desorption peak current follows the general trend of increasing in magnitude before tending to plateau (Figure 2e), as was reported for lysozyme,^[26a] haemoglobin^[29] and protamine.^[30] This indicates that there is a maximum amount of

adsorbed protein possible before the interface becomes saturated. In Figure 2e the coloured lines illustrate how the peak current reaches a plateau at lower concentrations as adsorption time increases. A linear increase of I_p with concentration was observed with increasing concentrations ($C_{\text{cyt } c} < 3 \mu\text{M}$) which presented greater sensitivity values (magnitude of the slope) when t_{ads} was increased from 0 to 120 s. On the other hand, longer interfacial adsorption times resulted in the appearance of additional features in the stripping voltammograms (Figure 2c). This effect impacts the peak current values presented in Figure 2f which do not follow the same trend as the data in Figure 2e. In Figure 2f, the linear range is decreased to the concentrations below $1 \mu\text{M}$. Under the conditions in Figure 2f ($E_{\text{ads}} = 0.975 \text{ V}$ and $t_{\text{ads}} = 300\text{s}$), a single desorption peak broadened at $C_{\text{cyt } c} = 2.5 \mu\text{M}$ and evolved into multiple peaks. This suggests that a different complexation/de-complexation mechanism occurs following interfacial saturation; this could be a direct consequence of changes occurring to protein-protein interactions and protein-anion complexes at these soft interface.

Figure 3a shows the AdSV of various concentrations of cyt c following adsorption at the optimized potential. It can be seen that as the concentration increases from $0.01 \mu\text{M}$ to $10.0 \mu\text{M}$ cyt c, the desorption peak changes from a single peak to double and triple peaks. This behaviour, not observed in lysozyme experiments,^[26] suggests the presence of multiple species on the interface or conformational changes of the protein and also reflects the altered behaviour observed (above) at longer preconcentration times (e.g. Figure 2c, f).

Study of cyt c at pure (i.e. not gelled) liquid/liquid water/1,2-dichloroethane (w/DCE) micro-interfaces also revealed unresolved peaks in the AdSV (Figure 3b), with similar trends with concentration as observed at the w/gelled-DCH interface. Interfacial coverages (Γ), calculated as elsewhere,^[16, 26a] were determined to track any relationship to the single, double and triple peaks (Figure 3).

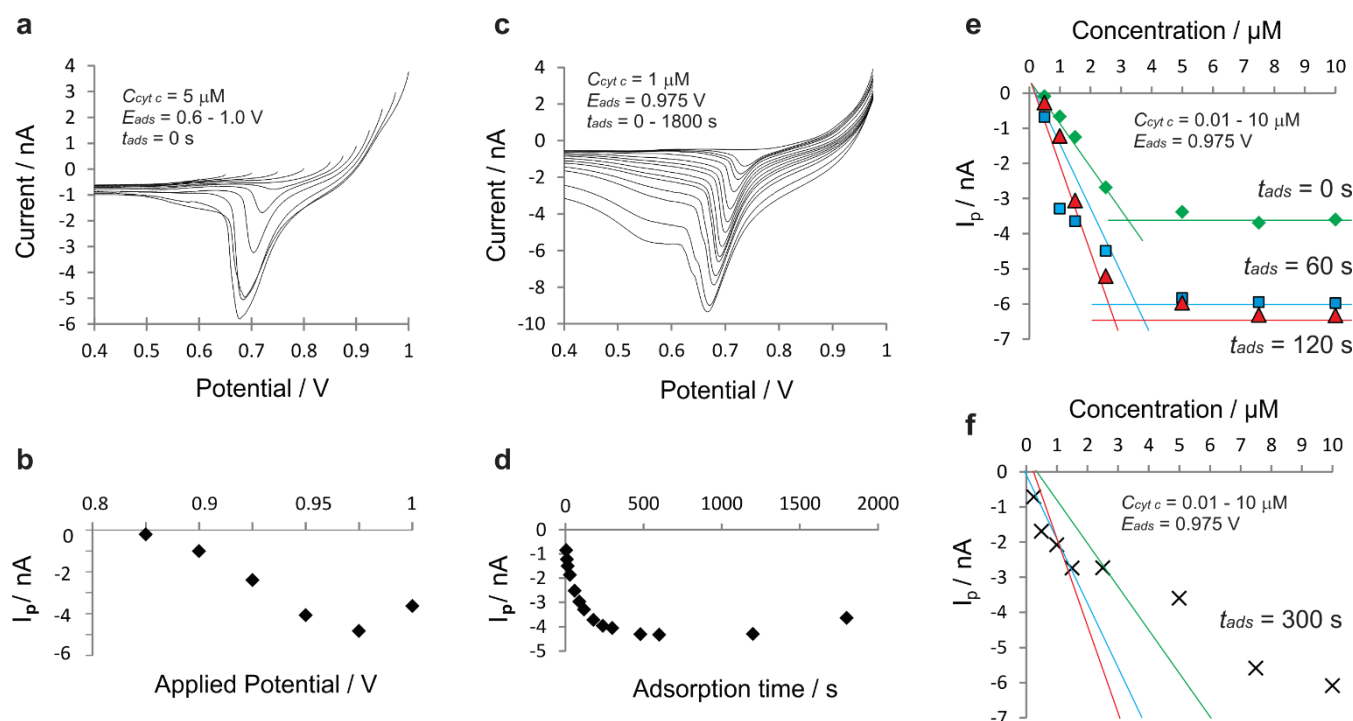


Figure 2. a) AdSV of $5 \mu\text{M}$ cyt c in 10 mM HCl following application of initial potentials in the range $0.6 \text{ V} - 1.0 \text{ V}$, at 5 mV s^{-1} and $t_{\text{ads}} = 0 \text{ s}$. b) Dependence of stripping peak current (I_p) on the initial applied potential ($\Delta_{\text{ap}}^{\text{ap}} E$), from measurements of peak heights in part (a). c) AdSV of $1 \mu\text{M}$ cyt c in 10 mM HCl at various adsorption times (0 to 1800 s) for a fixed adsorption potential (0.975 V). d) Dependence of I_p on t_{ads} . e) Peak current (I_p) versus concentration of cyt c ($0.01 - 10.0 \mu\text{M}$) for (♦) 0 s , (■) 60 s , (Δ) 120 s and f) (x) 300 s adsorption times. The coloured lines in (e) are a guide to the eye for the indicated concentrations; the linear portions of these lines are reproduced in (f) for comparison.

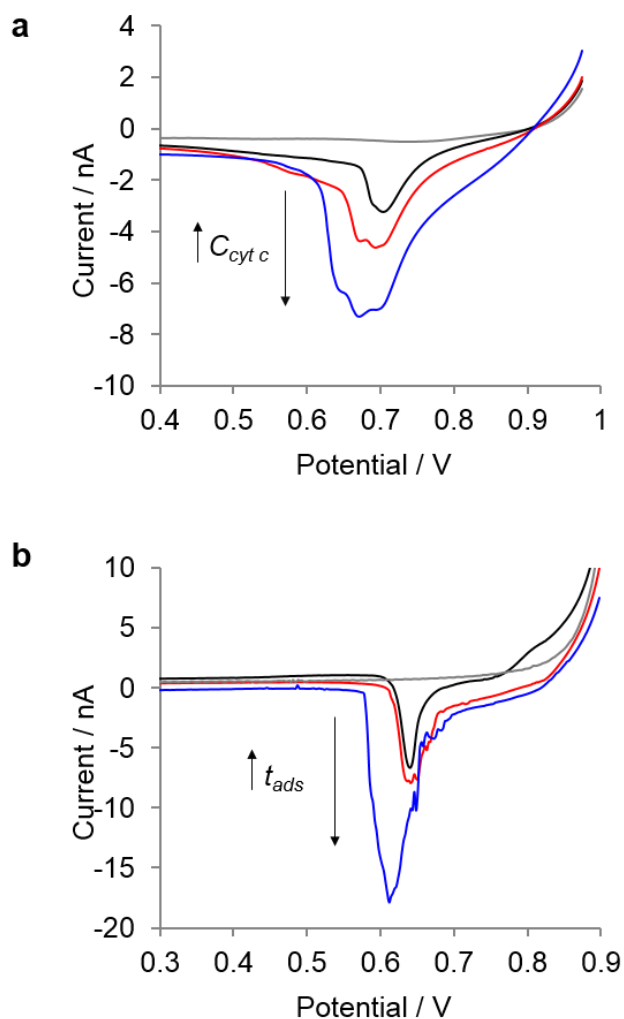


Figure 3. a) AdSV of various cyt *c* concentrations; $C_{\text{cyt } c} = 1.0 \mu\text{M}$ (—), $1.5 \mu\text{M}$ (—) and $7.5 \mu\text{M}$ (—), $E_{\text{ads}} = 0.975 \text{ V}$ and $t_{\text{ads}} = 300 \text{ s}$ at w/gelled-DCH. b) AdSV of $10.0 \mu\text{M}$ cyt *c*, $E_{\text{ads}} = 0.90 \text{ V}$ and $t_{\text{ads}} = 0 \text{ s}$ (—), 300 s (—) and 600 s (—) at w/DCE. Grey lines = absence of cyt *c*. Aqueous phase = 10 mM HCl . The arrows inserted in the voltammograms indicate that as the concentration $C_{\text{cyt } c}$ or adsorption time t_{ads} increased, the magnitude of the peak current increased.

These provided Γ values of 56, 141 and 420 pmol cm^{-2} for the 1.0, 1.5 and $7.5 \mu\text{M}$ cyt *c* peaks (Figure 3a, $t_{\text{ads}} = 300 \text{ s}$). Additionally the dependence on t_{ads} showed Γ values of 133, 221 and 628 pmol cm^{-2} for the 0, 300 and 600 s for $10 \mu\text{M}$ cyt *c* (Figure 3b, $C_{\text{cyt } c} = 10 \mu\text{M}$). This shows that similar impacts on the voltammetry were observed for both ITIES systems when the interfacial protein concentration was modulated by $C_{\text{cyt } c}$ or t_{ads} . Since cyt *c* is the only protein present in the system, a possible explanation for this unique behaviour is that protein-protein interactions, which become more likely at higher surface coverages, are affecting the complexation or de-complexation of the organic anion, leading to alterations in the stripping peak potentials. Cyt *c* is known to form dimers, trimers, tetramers and higher order oligomers under certain conditions;^[2, 5b, 31] perhaps the combination of acidic aqueous phase, interfacial complexation of organic electrolyte anion, and adsorption of the complex at the interface leads to conditions that promote such oligomerisation. Previous work illustrated the partial unfolding of lysozyme at soft interfaces (w/gelled-DCH) when this protein was electrochemically

adsorbed.^[27] Cyt *c* can undergo more extensive unfolding as it is less stabilised by disulfide bonds than lysozyme. The exposure of the hydrophobic amino acids of cyt *c* at the organic-aqueous interface may then lead to greater protein-protein and protein-anion interactions.

2.2. SDS-PAGE of cytochrome c aggregates

In order to investigate whether protein oligomers or polymers were formed at the interface during the electrochemical experiments, characterization of the electroadsorbed protein materials was undertaken by sodium dodecyl sulfate-polyacrylamide gel electrophoresis (SDS-PAGE) for size-based separation of protein species.^[32] Initially, cyt *c* was treated in various ways to induce oligomerization (pH 2, 7.4 or 9, at 25 or 75 °C for 16 h, results in Figure SI-1a). Thermal treatment was aimed at the formation of aggregates reported to occur at pH 9.^[1a] A wide band at 14.3 kD corresponding to cyt *c*^[32a] was observed following treatments at different pH values (25 °C). However, it was only after incubation at 75 °C and pH 9 that larger species were detected (27.1 kD (dimer) and 35.7 kD (trimer), Figure SI-1).

As the minimum amount of protein detectable via SDS-PAGE is greater than the amount preconcentrated at the microITIES array employed^[27] for the electrochemical measurements, larger interfaces were prepared so as to accumulate sufficient protein for SDS-PAGE analysis. Figure 4 summarizes the SDS-PAGE results obtained for the two ITIES: w/gelled-DCH (Figure 4a-b, Figure 4d lanes 1-3) and w/DCE (Figure 4c, Figure 4d lanes 4-6).

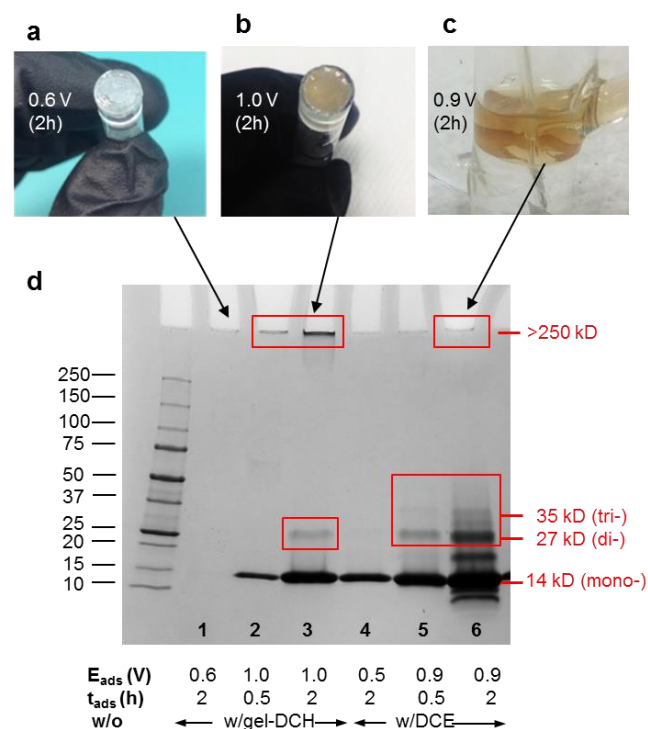


Figure 4. Images of the interface after 2 h electroadsorption at the w/gelled-DCH at a) 0.6 V, b) 1.0 V, and c) at w/DCE 0.9 V. d) SDS-PAGE of electroadsorbed material. $100 \mu\text{M}$ cyt *c*, electroadsorbed from 10 mM HCl (pH 2) at 25 °C to interfaces formed with either gelled-DCH (lanes 1-3) or liquid DCE (lanes 4-6), t_{ads} (0.5 or 2 h) and E_{ads} (no adsorption: 0.6 and 0.5 V; adsorption: 1.0 and 0.9 V) as indicated.

As a control experiment, electroadsorption was also implemented at a potential where there was no charge

transfer reaction (0.6 or 0.5 V) (Figure 4d, lanes 1 & 4). Figure 4a shows a colourless organogel (gelled-DCH) surface after 2h of electroadsorption at 0.6 V. This is in agreement with the absence of a band in lane 1 (Figure 4d), as adsorption is not promoted at this applied potential. The appearance of a band at 14.3 kD (cyt c monomer) in lane 4 is an artefact from sampling of the liquid w/DCE interface, as portions of both phases were taken and the aqueous phase contained 100 μ M cyt c. When the applied potential was sufficient to promote interfacial adsorption (1.0 V for w/gelled-DCH and 0.9 V for w/DCE), a brown film was observed on the surface of the organogel and SDS-PAGE revealed new bands at larger molecular weights (Figure 4b, Figure 4d lanes 3 & 6).

Two bands corresponding to 26.7 and >250 kD are shown in Figure 4d (lane 3) for cyt c recovered from the w/gelled-DCH interface; these correspond to dimeric and oligomeric species. Surprisingly, at the w/DCE interface a larger number of oligomers were observed by SDS-PAGE which correspond to cyt c dimers (27.0 kD), trimers (35.0 kD) and intermediate species, which might be protein bound to the organic electrolyte (~1 kD) or to degraded protein.

The differences in SDS-PAGE results for the water-organogel and pure liquid/liquid systems can be rationalised by the different sample recovery methods used with the w/gelled-DCH and w/DCE interfaces; the latter was more efficient and provided a larger amount of protein for analysis. When the film formed by 2 h adsorption at 0.9 V (w/DCE) (Figure 4c, Figure 4d lane 6) was re-suspended for SDS-PAGE, the dark brown film became milky brown, supportive of the presence of a significant amount of the organic phase electrolyte.

A qualitative analysis of Figure 4d reveals how both t_{ads} and E_{ads} drive the oligomerisation process. A trend in the formation of larger species with increasing t_{ads} and E_{ads} is evident. The increase in time results in a larger amount of oligomeric protein species (enhanced band intensity), in agreement with the trend observed in alkaline solution conditions (Figure SI-1c).

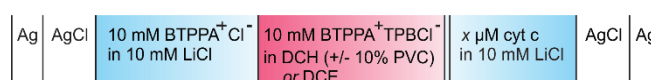
3. Conclusions

The electroactivity of cyt c was investigated at liquid/gel and liquid/liquid interfaces by adsorptive stripping voltammetry. The effects of adsorption time and bulk concentration of cyt c were investigated as well as the optimum adsorption potential. It was found that at longer adsorption times, which result in larger concentration of adsorbed protein, a single voltammetric response developed into a double and then a triple peak. Subsequent analysis of these protein films by SDS-PAGE revealed the presence of oligomeric structures (27, 35 and >250 kD) at the studied interfaces. This result is attributed to the formation of oligomeric species resulting from the unfolding of cyt c at the interface. Accordingly, these results provide the basis to use electrochemistry at soft interfaces as a platform to study the formation and inhibition of protein oligomers. Future scrutiny at the molecular level may provide insight in the mechanism of in this electrochemically-induced oligomerisation process.

Experimental Section

Reagents. All the reagents were purchased from Sigma-Aldrich Australia Ltd. and used as received, unless indicated otherwise. The organic phase was prepared using bis(triphenylphosphoranylidene) tetrakis (4-chlorophenyl)borate (BTTPA⁺TPBCl⁻, 10 mM) in 1,2-dichloroethane (DCE) or gelled-1,6-dichlorohexane (gelled-DCH) by adding 10 %m/v low molecular weight poly(vinyl chloride) (PVC) in the mixture.^[13a] The organic phase electrolyte salt BTTPA⁺TPBCl⁻ was prepared by metathesis of bis(triphenylphosphoranylidene)ammonium chloride (BTTPA⁺Cl⁻) and potassium tetrakis (4-chlorophenyl) borate (K⁺TPBCl⁻).^[33] Aqueous electrolyte solutions (10 mM HCl, 10 mM PBS, 50 mM TrisHCl) and aqueous stock solutions of cytochrome c (from equine heart) were prepared on a daily basis and stored at +4 °C. All the aqueous solutions were prepared in purified water (resistivity: 18.2 M Ω cm) from a USF Purelab Plus UV.

Electrochemical experiments. The electrochemical experiments were performed using an Autolab PGSTAT302N electrochemical analyser (Metrohm Autolab, Utrecht, The Netherlands), controlled by the NOVA software supplied with the instrument. A silicon membrane with 30 micropores etched in a hexagonal array was used to hold the soft microinterfaces. The micropore array fabrication^[34] provided pores with hydrophobic walls, with a 22.4 μ m diameter and a pore centre-to-centre distance of 400 μ m, giving a total geometric interface area of 1.2×10^{-4} cm². These microporous silicon membranes were sealed onto the lower orifice of a glass cylinder using silicone rubber (Acetic acid curing Selleys glass silicone). Then the organic phase (either DCE, DCH or 10%w/v PVC-DCH) was introduced into the silicon micropore arrays via the glass cylinder, and the organic reference solution was placed on top of the organic phase. The silicon membrane was then inserted into the aqueous phase. Voltammetric experiments were performed next, as previously described.^[17] The setup used for the experiments comprised of a 2 electrode cell,^[35] with one Ag|AgCl electrode in the organic phase and one in the aqueous phase. The cell utilised in these experiments is shown in Scheme 1, where x refers to the concentration of Cyt c. All potentials are reported with respect to the experimentally-used reference electrodes. Cyclic voltammetry (CV) and adsorptive stripping voltammetry (AdSV) were carried out at a sweep rate of 5 mV s⁻¹ and parameters such as protein concentration, applied potential, and duration of the adsorption stage were varied. For AdSV, the potential was stepped from open-circuit to the chosen adsorption potential, held at that potential for the chosen time, and then scanned from the adsorption potential to final potential.



Scheme 1. Electrochemical cell employed to accumulate cytochrome c at the soft (liquid-liquid or liquid-gel) interface. Blue is aqueous solution and red is the organic phase.

A larger interfacial area (2.69 cm²) was required to accumulate a sufficient amount of protein prior to SDS-PAGE analyses, thus 2 Pt counter electrodes and 2 Ag/AgCl electrodes (one of each in each phase) were used to control the electrochemical experiments in these cases. This was achieved by using a single interface which was formed in a 4-electrode glass cell ($r = 0.93$ cm).

Aggregation assays in solution. Samples containing 100 μ M cyt c were incubated for 16 h at 75 °C at pH 9 (0.05 M TrisHCl) to promote aggregation.^[1a] Controls were performed at 25 °C in pH 2 (10 mM HCl) and 7.4 (10 mM PBS).

Electrochemical aggregation prior to SDS-PAGE. Larger interfaces were employed; 1.06 (w/gelled-DCH) - 2.69 (w/DCE) cm² for SDS-PAGE. For SDS-PAGE, 100 μ M cyt c was electrochemically adsorbed, then the gel was removed with a scalpel as reported previously^[27] and dissolved with the loading buffer (Scheme SI-1).

Sodium dodecyl sulfate polyacrylamide gel electrophoresis (SDS-PAGE). The protein aggregates were resolved by SDS-PAGE (4-20% Mini-Protean pre-casted gels from BioRad) at 200 V (30 min) for 30 μ L of sample loaded per well (3 μ L protein sample in 30 μ L loading buffer). The loading buffer was Laemmli buffer (65.8 mM Tris-HCl, pH 6.8, 2.1% SDS, 26.3% w/v glycerol and 0.01% bromophenol blue) whilst the running buffer was 25 mM Tris + 192 mM glycine and 0.1 % SDS. Reducing conditions were carried out by adding 5% (v/v) of β -mercaptoethanol in the loading buffer. The gels were stained with 0.08% Coomassie Brilliant Blue G250, 1.6% ortho-phosphoric acid, 8% ammonium sulfate and 20% methanol and de-stained with 10% acetic acid in 50/50 water/methanol before imaging. The protein standards (10 – 250 KD) were purchased from BioRad (Precision Plus Protein Standards) and an individual calibration curve (log molecular weight vs relative front, Rf) was generated for each individual gel.

UV/vis spectroscopy. Ultraviolet/visible (UV/vis) absorbance spectroscopy was carried out using a Perkin-Elmer Lambda 35 instrument. The instrument was scanned in the range of 250 nm to 700 nm at 480 nm min^{-1} . The slit width was 1 nm with a resolution of 1 nm. The sample was placed in a 1 x 1 cm quartz cuvette. Figure SI-2 shows the cytochrome c spectra in water and 10 mM HCl.

Acknowledgements

EAdE and SOS thank Curtin University for the award of PhD scholarships. The authors thank the Curtin Health Innovation Research Institute for access to electrophoretic apparatus.

Keywords: protein • oligomerisation • liquid-liquid interfaces • electrochemistry • adsorption

- [1] a N. S. de Groot, S. Ventura, *Spectroscopy* **2005**, *19*, 199-205; b Y. P. Ow, D. R. Green, Z. Hao, T. W. Mak, *Nat. Rev. Mol. Cell Biol.* **2008**, *9*, 532-542.
- [2] a E. Margoliash, J. Lustgarten, *The Journal of biological chemistry* **1962**, *237*, 3397-3405; b A. Schejter, S. C. Glauser, P. George, E. Margoliash, *Biochimica et Biophysica Acta (BBA) - Specialized Section on Enzymological Subjects* **1963**, *73*, 641-643.
- [3] S. Hirota, Y. Hattori, S. Nagao, M. Taketa, H. Komori, H. Kamikubo, Z. H. Wang, I. Takahashi, S. Negi, Y. Sugiura, M. Kataoka, Y. Higuchi, *Proc. Natl. Acad. Sci. U. S. A.* **2010**, *107*, 12854-12859.
- [4] F. Chiti, C. M. Dobson, in *Annual Review of Biochemistry*, Vol. 75, Annual Reviews, Palo Alto, **2006**, pp. 333-366.
- [5] a G. Balakrishnan, Y. Hu, O. F. Oyerinde, J. Su, J. T. Groves, T. G. Spiro, *J. Am. Chem. Soc.* **2007**, *129*, 504-505; b T. Konno, *Protein Science* **1998**, *7*, 975-982; c G. Balakrishnan, Y. Hu, T. G. Spiro, *J. Am. Chem. Soc.* **2012**, *134*, 19061-19069.
- [6] a S. M. Singh, J. Cabello-Villegas, R. L. Hutchings, K. M. Mallela, *Proteins* **2010**, *78*, 2625-2637; b S. Haldar, P. Sil, M. Thangamuniyandi, K. Chattopadhyay, *Langmuir* **2015**, *31*, 4213-4223; c I. W. Hamley, *Nat. Chem.* **2010**, *2*, 707-708.
- [7] a O. S. Makin, E. Atkins, P. Sikorski, J. Johansson, L. C. Serpell, *Proc. Natl. Acad. Sci. U. S. A.* **2005**, *102*, 315-320; b W. Pulawski, U. Ghoshdastider, V. Andrisano, S. Filipek, *Appl. Biochem. Biotechnol.* **2012**, *166*, 1626-1643; c L. N. Mironova, A. I. Goginashvili, M. D. Ter-Avanesyan, *Mol. Biol.* **2008**, *42*, 710-719.
- [8] a M. Sunde, C. C. F. Blake, *Q. Rev. Biophys.* **1998**, *31*, 1-+; b J. Khoshnoodi, J. P. Cartailier, K. Alvares, A. Veis, B. G. Hudson, *Journal of Biological Chemistry* **2006**, *281*, 38117-38121.
- [9] B. Caughey, P. T. Lansbury, *Annu. Rev. Neurosci.* **2003**, *26*, 267-298.
- [10] A. Veloso, K. Kerman, *Anal. Bioanal. Chem.* **2013**, *405*, 5725-5741.
- [11] a P. Lopes, M. Xu, M. Zhang, T. Zhou, Y. L. Yang, C. Wang, E. E. Ferapontova, *Nanoscale* **2014**, *6*, 7853-7857; b P. Lopes, E. E. Ferapontova, *Monatshfte für Chemie - Chemical Monthly* **2015**, *146*, 781-786.
- [12] D. W. M. Arrigan, *Anal. Lett.* **2008**, *41*, 3233-3252.
- [13] a M. D. Scanlon, G. Herzog, D. W. M. Arrigan, *Anal. Chem.* **2008**, *80*, 5743-5749; b G. Herzog, D. W. M. Arrigan, *Analyst* **2007**, *132*, 615-632.
- [14] G. Herzog, V. Kam, D. W. M. Arrigan, *Electrochim. Acta* **2008**, *53*, 7204-7209.
- [15] G. C. Lillie, S. M. Holmes, R. A. W. Dryfe, *J. Phys. Chem. B* **2002**, *106*, 12101-12103.
- [16] S. O'Sullivan, D. W. M. Arrigan, *Electrochim. Acta* **2012**, *77*, 71-76.
- [17] M. D. Scanlon, E. Jennings, D. W. M. Arrigan, *Phys. Chem. Chem. Phys.* **2009**, *11*, 2272-2280.
- [18] a M. D. Scanlon, J. Strutwolf, D. W. M. Arrigan, *Phys. Chem. Chem. Phys.* **2010**, *12*, 10040-10047; b M. D. Scanlon, D. W. M. Arrigan, *Electroanalysis* **2011**, *23*, 1023-1028; c A. Berduque, R. Zazpe, D. W. M. Arrigan, *Anal. Chim. Acta* **2008**, *611*, 156-162.
- [19] a J. A. Ribeiro, I. M. Miranda, F. Silva, C. M. Pereira, *Phys. Chem. Chem. Phys.* **2010**, *12*, 15190-15194; b S. N. Faisal, C. M. Pereira, S. Rho, H. J. Lee, *Phys. Chem. Chem. Phys.* **2010**, *12*, 15184-15189; c J. D. Guo, Y. Yuan, S. Amemiya, *Anal. Chem.* **2005**, *77*, 5711-5719.
- [20] a E. Gohara, T. Osakai, *Anal. Sci.* **2010**, *26*, 375-378; b R. Matsui, T. Sakaki, T. Osakai, *Electroanalysis* **2012**, *24*, 1164-1169.
- [21] a M. Shinshi, T. Sugihara, T. Osakai, M. Goto, *Langmuir* **2006**, *22*, 5937-5944; b T. Osakai, Y. Yuguchi, E. Gohara, H. Katano, *Langmuir* **2010**, *26*, 11530-11537; c Y. Imai, T. Sugihara, T. Osakai, *The Journal of Physical Chemistry B* **2012**, *116*, 585-592.
- [22] G. Herzog, P. Eichelmann-Daly, D. W. M. Arrigan, *Electrochem. Commun.* **2010**, *12*, 335-337.
- [23] J. Zhai, S. V. Hoffmann, L. Day, T.-H. Lee, M. A. Augustin, M.-I. Aguilar, T. J. Wooster, *Langmuir* **2011**.
- [24] R. A. Hartvig, M. van de Weert, J. Ostergaard, L. Jorgensen, H. Jensen, *Langmuir* **2012**, *28*, 1804-1815.
- [25] R. A. Hartvig, M. A. Mendez, M. van de Weert, L. Jorgensen, J. Ostergaard, H. H. Girault, H. Jensen, *Anal. Chem.* **2010**, *82*, 7699-7705.
- [26] a E. Alvarez de Eulate, D. W. M. Arrigan, *Anal. Chem.* **2012**, *84*, 2505-2511; b B. M. Felisilda, E. Alvarez de Eulate, D. W. Arrigan, *Anal. Chim. Acta* **2015**, *893*, 34-40.
- [27] E. Alvarez de Eulate, L. Qiao, M. D. Scanlon, H. H. Girault, D. W. M. Arrigan, *Chem. Commun.* **2014**, *50*, 11829-11832.
- [28] L. Malmgren, Y. Olsson, T. Olsson, K. Kristensson, *Brain Res.* **1978**, *153*, 477-493.
- [29] E. Alvarez de Eulate, L. Serls, D. W. M. Arrigan, *Anal. Bioanal. Chem.* **2013**, *405*, 3801-3806.
- [30] M. B. Garada, B. Kabagambe, S. Amemiya, *Anal. Chem.* **2015**, *87*, 5348-5355.
- [31] S. Dupr, M. Brunori, C. Greenwood, M. T. Wilson, *Biochemical journal* **1974**, *141*, 299-304.
- [32] a M. Hashimoto, A. Takeda, L. J. Hsu, T. Takenouchi, E. Masliah, *J. Biol. Chem.* **1999**, *274*, 28849-28852; b K. Weber, M. Osborn, *J. Biol. Chem.* **2006**, *281*.
- [33] H. J. Lee, P. D. Beattie, B. J. Seddon, M. D. Osborne, H. H. Girault, *J. Electroanal. Chem.* **1997**, *440*, 73-82.
- [34] R. Zazpe, C. Hibert, J. O'Brien, Y. H. Lanyon, D. W. M. Arrigan, *Lab Chip* **2007**, *7*, 1732-1737.
- [35] T. Osakai, T. Kakutani, M. Senda, *B Chem Soc Jpn* **1984**, *57*, 370-376.

